CrossMark

ORIGINAL PAPER

A Wear Rule and Cutter Life Prediction Model of a 20-in. TBM Cutter for Granite: A Case Study of a Water Conveyance Tunnel in China

Quansheng Liu[1,2] · Jianping Liu[1,3] · Yucong Pan[1,3] · Xiaoping Zhang[2] ·
Xingxin Peng[1,3] · Qiuming Gong[4] · Lijie Du[5]

Abstract Disc cutter wear is one of the comprehensive results of the rock–machine interaction in tunnel boring machine (TBM) tunneling. The replacement of the disc cutter is a time-consuming and costly activity that can significantly reduce the TBM utilization (U) and advance rate (AR), and has a major effect on the total time and cost of TBM tunneling projects. Therefore, the importance of predicting the cutter life accurately can never be overemphasized. Most cutter wear prediction models are only suitable for 17-in. or smaller disc cutters. However, use of large-diameter disc cutters has been an irresistible trend for large-section hard rock TBMs. This study attempts to reveal the genuine wear rule of a 20-in. disc cutter and develop a new empirical model for predicting the cutter life in granite based on field data collected from a water conveyance tunnel constructed by the TBM tunneling method in China. The field data including the actual cutter wear and the geological parameters along the studied tunnel were compiled in a special database that was subjected to statistical analysis to reveal the genuine wear rule of a 20-in. disc cutter and develop the reasonable correlations between some common intact rock parameters and the disc cutter life. These equations were developed based on data from massive to very massive granite with a UCS range of 40–100 MPa, which can be applied for the assessment of the cutter life of a 20-in. disc cutter in similar hard rock projects with similar rock strengths and rock abrasivities.

1 Introduction

Disc cutters are indispensable tools for various types of tunnel excavation equipment from pipe jacking micro-TBMs with diameters less than 1 m to hard rock macro-TBMs with diameters larger than 14 m. The first successful use of a TBM was for the Oahe Dam project in South Dakota, where the machine excavated faulted and jointed shale at only 1–3 MPa with a Robbins main beam TBM 910–101 in 1952 (Roby et al. 2008). In the early days, TBMs were employed primarily in weak to moderate strength rocks that can be excavated with low cutter loads. Hence, the disc cutters were of small size, which made them easy to transport and replace. However, hard rocks with uniaxial compressive strengths (UCS) up to 400 MPa were encountered by the TBMs, which resulted in unacceptable cutter wear rates and costs with small disc cutters.

Replacing worn cutters is very costly. When a disc cutter must be changed in an excavation stroke, the contractor incurs the cost of downtime as well as the cost of

✉ Jianping Liu
  jpliu_whrsm@foxmail.com

[1] State Key Laboratory of Geomechanics and Geotechnical Engineering, Institute of Rock and Soil Mechanics, Chinese Academy of Sciences, Wuhan, China

[2] Key Laboratory of Safety for Geotechnical and Structural Engineering of Hubei Province, School of Civil Engineering, Wuhan University, Wuhan, China

[3] University of Chinese Academy of Sciences, Beijing, China

[4] Key Laboratory of Urban Security and Disaster Engineering of Ministry of Education, Beijing University of Technology, Beijing, China

[5] Key Laboratory of Structural Health Monitoring and Control of Hebei Province, Shijiazhuang Tiedao University, Shijiazhuang, China

refurbishing or replacing the disc cutter (Roby et al. 2008). Therefore, the cutter cost represents a large portion of the total construction cost in TBM tunneling projects, for example approximately one-third in the Qinling TBM tunneling project in China (Wan et al. 2002a). To reduce the cutter wear rate and cutter cost in TBM tunneling, disc cutter manufacturers have attempted to use various methods to improve the cutter life. Increasing the ratio of cutter re-ringing to rebuilding allows maintaining the lowest consumable cost in projects through using improved lubricants and keeping a precise record. On the other hand, increasing the available wear volume of the cutter ring, the most cost-effective way, can reduce downtime for cutter changing, which means more time available for TBM boring. To meet the excavation requirements in hard rock, the cutter diameter and its corresponding load capacity have been constantly enlarged over the years, as shown in Table 1 (Roby et al. 2008). A main beam hard rock TBM with a 14.4 m diameter was the first ever to be fitted with 20-in. cutters and was used for the excavation of the tunnels in the Canadian Niagara hydroelectric power project in 2006.

Researchers' access to data relevant to cutter wear has been restricted until now, as these sensitive data are dealt with discretely by TBM manufacturers or tunnel construction firms (Schneider et al. 2012). Therefore, there are few reports on the wear rule of disc cutters in the accessible literatures. Wei and Sha (1999) and Wan et al. (2002b) analyzed the cutter wear rule in migmatitic granite and amphogneiss based on the actual cutter wear data of 3688- and 5621-m tunnel sections in the Qinling TBM tunneling project in China, respectively. Jin et al. (2011) counted the number of disc cutter changes with each cutter position in a 5938-m section of the 9# tunnel of the Yintao project in China. Hassanpour et al. (2014) analyzed the cutter wear data of the Karaj water conveyance tunnel covering approximately 30 km in Iran. Zhao (2015) discussed the number of disc cutter changes with each cutter position

based on the cutter change reports of a section of 4968 m in the West Qinling railway tunnel in China. Du et al. (2015) studied the cutter wear rule of each cutter position and the correlation of the cutter wear with the rock mass classification based on the daily cutter wear records of a 4167-m tunnel section in China.

Cutter wear has always and will always represent a cost-intensive and performance-critical factor for rock excavation. Cutter wear not only directly influences a project, e.g., through cutter and personnel costs related to replacing worn cutters, but it can also influence the working cycle and the performance of the rock excavation process (Plinninger 2010). Therefore, the significance of predicting the cutter life accurately in different conditions can never be overemphasized. The use of a new generation of large-diameter hard rock TBMs, which started in many countries simultaneously in the 1990s, was good reason to revisit the problem of forecasting cutter wear (Schneider et al. 2012). The most commonly used models for predicting cutter wear are the CSM model (Rostami 1997), NTNU model (Bruland 1998), and Gehring model (Gehring 1995). Hassanpour et al. (2014) summarized the common cutter wear prediction models, and developed an empirical TBM cutter wear prediction model for pyroclastic and mafic igneous rocks. In addition to the models mentioned by Hassanpour et al. (2014), the works done by Wijk (1992), Dahl et al. (2007), Wang et al. (2012), and Yang et al. (2015) are also attempts to develop cutter wear prediction models. Wijk (1992) assumed that the disc cutter rolling distance is proportional to the volume of steel worn off the cutter and is inversely proportional to the cutter pressure on the rock and then obtained mathematical formulas for the cutter life of two different types of cutter, namely the wedge-shaped cutter and constant cross-sectional (CCS) cutter. Dahl et al. (2007) attempted to estimate the cutter life based on the updated Sievers' J miniature drill test. The point in time at which an interception occurs between the tangent lines to what could be defined as the "effective drilling" part and the "worn out" part of the penetration curve is defined as the Sievers' J interception point, or SJIP. Testing results show that it is possible to obtain a direct cutter life estimate by the use of SJIP. Wang et al. (2012) established a novel energy method based on the specific energy (SE) rule and wear mechanism. The average wear extent of all disc cutters on the hard rock TBM cutterhead can be calculated using the SE equations, and the wear extent of any disc cutter can be predicted according to the wear mechanism and layout of the disc cutters on the cutterhead. Yang et al. (2015) developed prediction models for the cutter wear rate and linear wear rate by approximate calculation and mathematical deduction based on the Rabinowicz equation and CSM model. The normal cutting distance of disc cutters with various layout radiuses can be predicted by the

Table 1 Variations of cutter diameters and load capacities over time (from Roby et al. 2008)

Diameter (in.)	Load (kN)	Year introduced
11	85	1961
12	125	1969
13	145	1980
14	165	1976
15.5	200	1973
16.25	200	1987
17	215	1983
19	312	1989
20	312	2006

cutter wear rate prediction model, and the linear wear rate can be taken as an indicator of the abrasivity of the excavated rocks.

The disc cutter wear is influenced by two different groups of factors, namely geological conditions (including the intact rock parameters, rock mass parameters, and environmental factors) and TBM operating parameters (including the cutterhead rotation speed and thrust) (Frenzel et al. 2008). The existing disc cutter wear prediction models are shown in Table 2. However, it is indisputable that the accuracy of the disc cutter wear prediction models is not currently satisfactory. This is best explained by Schneider et al. (2012): ''these models are mostly based on correlations with a wear coefficient, e.g., the Cerchar abrasivity index, and they deliver highly variable results'' or by Hassanpour et al. (2014): ''the most important problem in most of these models is their consideration of only one abrasivity parameter in the model as the input

parameter and ignoring the effects of other important parameters such as the rock strength and rock mass fracturing degree and structure.'' In addition, most of these models are only suitable for 17-in. or smaller disc cutters. However, the use of large-diameter disc cutters has been an irresistible trend for large-section hard rock TBMs (Du 2006; Du et al. 2015; Liu et al. 2016a), as they have many advantages. First, although the contact area between the rock and disc cutter is larger during TBM tunneling, which leads to a smaller penetration at the same equivalent thrust per cutter, the load capacity is significantly improved, as shown in Table 1, which can offset this drop in penetration. Second, the available cutter ring wear volume of the large-diameter disc cutter is improved, e.g., compared with the available cutter ring wear volume of the 17-in. disc cutter, those of the 19- and 20-in. disc cutters are increased by 38 and 218%, respectively, which leads to less downtime for the cutter replacement, such that the efficiency of the TBM

Table 2 Existing disc cutter wear prediction models (modified from Hassanpour et al. 2014)

No.	References	Required geomechanical tests	Input geomechanical parameters	Output cutter wear parameters
1	Ewendt (1992)	Petrographic analysis and point load test	Quartz content, grain size, and point load index	Wear rate
2	Wijk (1992)	Cerchar abrasivity test, uniaxial compressive strength (UCS) test, and point load test	Cerchar abrasivity index (CAI), UCS, tensile strength (σ_{PLT})	Rolling distance
3	Nelson et al. (1994)	–	–	Total cost, delays, and total number of changed cutters
4	Gehring (1995)	Cerchar abrasivity test and UCS test	CAI, UCS	Average cutter ring life
5	Rostami (1997)	Cerchar abrasivity test	CAI	Average rolling distance, total cost, delays, and total number of changed cutters
6	Bruland (1998)	Sievers' J miniature drill test and AVS test	Cutter life index (CLI)	Average cutter ring life, total cost, delays, and total number of changed cutters
7	Dahl et al. (2007)	Sievers' J interception point test	SJIP start, SJIP steepest	Cutter life index
8	Maidl et al. (2008)	Cerchar abrasivity test and UCS test	CAI, UCS	Average rolling distance
9	Bieniawski et al. (2009)	Cerchar abrasivity test, UCS test, brittleness test (S_{20}), and Sievers' J miniature drill test (SJ)	CAI, UCS, DRI	Specific cutter consumption
10	Frenzel (2011)	Cerchar abrasivity test	CAI	Net cutter life, total number of changed cutters, and total cost
11	Wang et al. (2012)	–	Specific energy of entire cutterhead (E_s)	Average wear extent and number of ineffective cutters
12	Hassanpour et al. (2014)	Vickers hardness test and UCS test	Vickers hardness number of rock (VHNR), UCS, ABI	Average cutter ring life
13	Yang et al. (2015)	UCS test	UCS	Wear rate and linear wear rate

tunneling is greatly improved. At the same time, the use of large-diameter disc cutters also has some shortcomings. The assembly weight of a large-diameter disc cutter is larger than that of a small-diameter disc cutter, which makes the former difficult to transport and replace. Additionally, the increased difference in the cutter ring wear extent between the new cutters and the worn cutters leads to greater loads assigned to the new ones due to their raised cutter rings, which may increase the ratio of abnormal wear to normal wear for large-diameter disc cutters.

As stated by Bruland (1998): ''due to the relative rapid development of the TBM technology, a prediction model for TBM tunneling should not be more than 8–10 years old before it is revised based on the new information available.'' Thus, during the construction phase of a TBM tunneling project in granite in China, a specific database including the actual cutter wear and geological data from different chainages of the studied tunnel was established and subjected to statistical analysis to reveal the genuine wear rule of a 20-in. disc cutter and develop reliable relationships between some common intact rock parameters and the disc cutter life. The new cutter wear prediction model can be applied for estimating the life of a 20-in. disc cutter in similar hard rock projects with similar rock strengths and rock abrasivities.

2 Project Description

A water conveyance tunnel with a total length of approximately 15.36 km, an excavation diameter of 8.50 m, and a longitudinal slope of 0.28‰ is selected for this study. The tunnel is divided into two sections, namely Lot 1 or A–B (8.83 km) and Lot 2 or B–C (6.50 km). The studied tunnel sections in this study include the whole Lot 1 and the first 1.0 km of Lot 2. The corresponding longitudinal geological profile along the studied tunnel is shown in Fig. 1. The overburden of the studied tunnel is all over 100 m, and the overburden of some sections below the peak is greater than 400 m. The hard rock lithology of the surrounding rock is slightly weathered granite of the Proterozoic era with a porphyritic texture and massive structure. The rock mass intactness degree is relatively integrated and poorly integrated with local relatively fractured in valley sections. The rock mass classifications of the studied tunnel, as shown in Fig. 2, are class II (accounting for approximately 81.28%), class IIIa (approximately 11.92%), class IIIb (approximately 4.27%), and class IV (approximately 2.53%), based on the Hydropower Classification (HC) method (The National Standards Compilation Group of People's Republic of China 2009). The Hydropower Classification (HC) method, commonly used for the evaluation of the overall stability of the surrounding rock, to guide excavation, and for the support

design of underground engineering in water conservancy and hydropower industry in China, is similar to the Rock Mass Rating (RMR) system (Bieniawski 1989). The intact rock strength, rock mass intactness degree, and discontinuity conditions are regarded as the basic influencing factors in the HC method, and all of them are assigned positive values. The groundwater condition and attitude of the major discontinuity plane are employed as correction factors and assigned negative values. These five factors will be subjected to an accumulation method to derive a composite index, namely the cumulative score T. The rock mass classification is synthetically determined by taking the strength–stress ratio S into consideration to integrate the effect of the stress state on the stability of the surrounding rock (The National Standards Compilation Group of People's Republic of China 2009). The rock mass classification of the HC method is shown in Table 3.

A gripper TBM manufactured by Robbins Company, as shown in Fig. 3, was employed to excavate the whole tunnel. The TBM assembly was accomplished in the A portal, and the TBM tunneling commenced on February 20, 2014. Lot 1, with a total length of approximately 9 km, was completed in 14 months (on April 21, 2015). The average monthly advance and TBM utilization of this segment were 630 m and 45.4%, respectively. The TBM continued to excavate Lot 2 on July 10, 2015 after being overhauled at the B portal. Lot 2, with a length of approximately 1.0 km, was finished on September 9, 2015.

3 Machine Specifications

The cutterhead is laced with 49 disc cutters, including 4 double-ring center cutters of diameter 17 in. or 432 mm, 35 single-ring face cutters of diameter 20 in. or 508 mm, and 10 single-ring gage cutters of diameter 20 in. or 508 mm. The other main specifications of the TBM are listed in Table 4.

The cutter number increases with the distance to the center of the cutterhead. Figure 4a shows a view of the cutterhead of the employed TBM at the B portal. Figure 4b shows the cutter arrangement on the cutterhead with the cutter numbers. The allowable wear limit of the disc cutter varies with the position and type of the disc cutter. In this study, after consideration of the cutter size, tunnel overexcavation, and cutterhead protection, the allowable wear limits of each center cutter and face cutter are determined to be 25 and 35 mm, respectively, and the allowable wear limits of the gage cutters with cutter Nos. 44–46, 47–51, and 52–53 are 25, 19, and 12 mm, respectively. In general, the TBM must be stopped routinely after each 3–4 excavation strokes to inspect the conditions of all disc cutters to ensure that the TBM can be operated
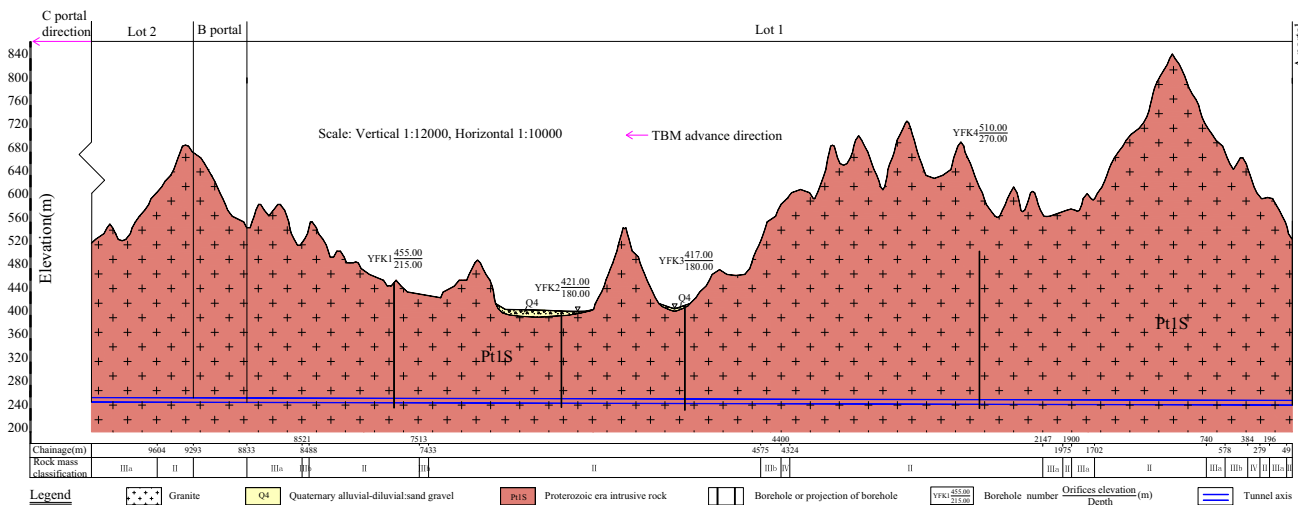
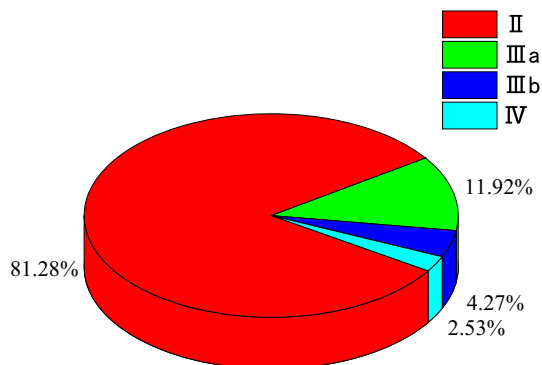**Fig. 1** Longitudinal geological profile along the studied tunnel

Fig. 2 Pie chart of rock mass classifications of the studied tunnel

Table 3 Rock mass classification based on HC method

Class	Cumulative score T	Strength–stress ratio S
I	$T > 85$	>4
II	$85 \geq T > 65$	>4
III	$65 \geq T > 45$	>2
IV	$45 \geq T > 25$	>2
V	$T \leq 25$	–

$T = A + B + C + D + E$, where A, B, C, D, E are the ratings of the intact rock strength, rock mass intactness degree, discontinuity conditions, groundwater condition, and the main discontinuity plane attitude, respectively. $S = R_c * K_v / \sigma_m$, where R_c is the uniaxial compressive strength of the intact saturated rock (MPa), K_v is the intactness index of the rock mass, and σ_m is the maximum principal stress of the surrounding rock (MPa), which could be replaced with the geostatic stress when no measured information is obtained in the field. When the strength–stress ratio S of the rock mass in classes I, II, III, and IV is less than the specified value in Table 3, the rock mass classification should be reduced by one grade

continually without cutters failure until the regularly scheduled maintenance. The wear extent of every disc cutter in units of millimeters is measured with a gage and
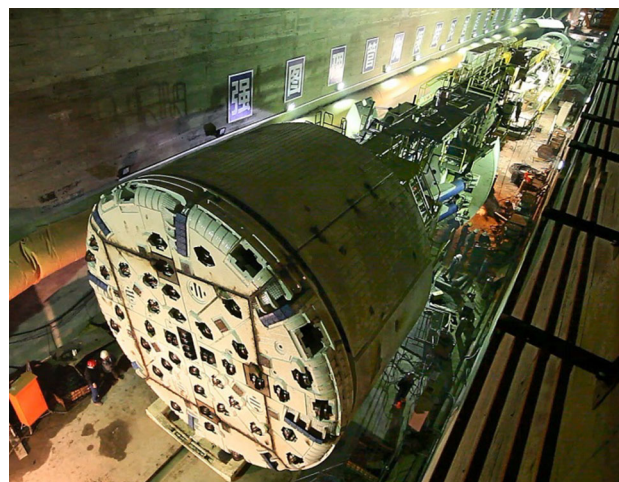

Fig. 3 Gripper TBM employed in this study

recorded in the daily TBM cutter maintenance sheet during the daily maintenance of the machine, as shown in Fig. 5. The reason for every disc cutter change is recorded at the same time. The cutters that reach their respective allowable wear limit or abnormal wear are replaced, and the worn cutters are adjusted properly to ensure that the difference in the cutter ring wear extent between adjacent cutters is less than 15 mm. The gage cutters that reach the corresponding allowable wear limit can continue to be used by being adjusted to the positions of the face cutters.

4 Evaluation Index of Disc Cutter Life

No uniform index has been confirmed for evaluating the disc cutter life, although various evaluation indices have been introduced and used by researchers. This includes
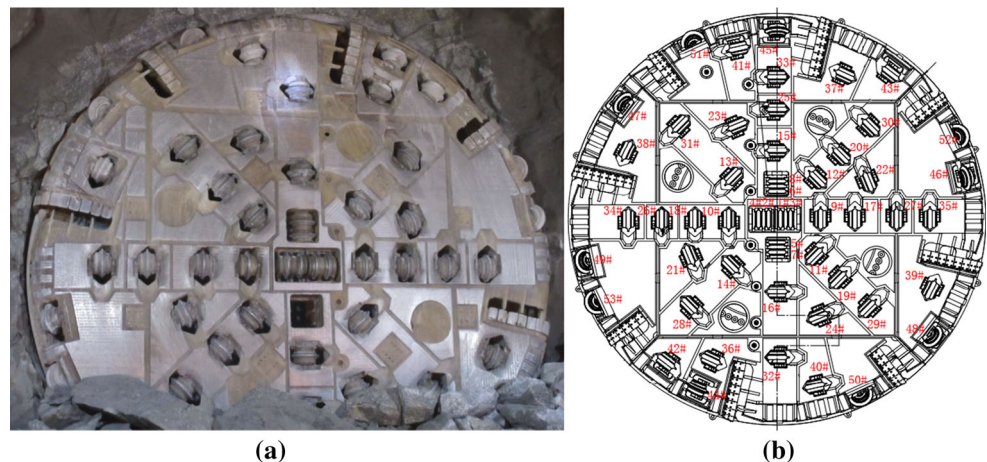
Table 4 Main specifications of the TBM in this study

Technical parameter	Design value
TBM model	Robbins MB280
TBM type	Open
TBM diameter (m)	8.5
Individual cutter nominal load (kN)	311.5
Cutter ring hardness (HRC)	58
Face cutter spacing (mm)	89
Cutterhead power (kW)	$10 \times 330 = 3300$
Rotational speed (rpm)	0–6.9
Cutterhead nominal torque (kN m)	6713
Cutterhead nominal thrust (kN)	16,509.5
Maximum allowable thrust (kN)	20,491 at 345 bar
Thrust cylinder stroke (mm)	1829
Conveyor capacity (t/h)	2196
TBM weight (tons)	Approx. 1375

Fig. 5 Manual measurement of cutter wear extent

hours used per cutter or H_h (h/cutter) (Bruland 1998), rolling distance per cutter or H_m (m/cutter) (Bruland 1998), rock excavation volume per cutter or H_f (m³/cutter) (Bruland 1998), cutter wear extent per rock excavation volume or V_f (mm/m³) (Wan et al. 2002b), rock excavation volume or V_c (m³) (Frenzel 2011, 2012), and cutter wear extent per rolling distance or V_m (mm/m) (Du et al. 2015).
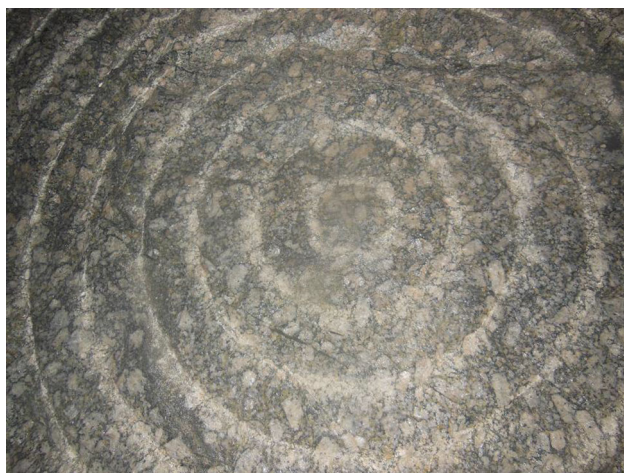
A series of concentric circles is produced on the tunnel face by the disc cutters during the TBM tunneling. As shown in Fig. 6, the movement track of every disc cutter is helical, namely with a combination of cutterhead rotation and a forward advance, as shown in Fig. 7. Therefore, the rolling distance of the disc cutter is closely linked to the position of the disc cutter and the penetration per revolution of the TBM cutterhead. However, the disc cutter life in the form of rolling distance per cutter or H_m (m/cutter) decreases with the increasing tunnel diameter in given

ground conditions. To ignore the influence of the tunnel diameter on the disc cutter life and make a possible comparison of the disc cutter life between different projects, the disc cutter life in the form of the rock excavation volume per cutter or H_f (m³/cutter) was introduced (Hassanpour et al. 2014). Unfortunately, the calculation of H_f (m³/cutter) is somewhat complicated and requires the application of a special software compiled by NTNU (Bruland 1998).

The rock fragmentation efficiency by a wedge disc cutter decreases rapidly due to the increasing contact width between the disc cutter and rock with the wear of the cutter ring. However, the CCS disc cutter shows little change in contact width before and after wear, which means that the rock fragmentation efficiency of the CCS disc cutter is far more stable. Thus, CCS disc cutters have been widely used in TBM tunneling since the 1970s (Liu et al. 2016b). As noted earlier, the wear extent of every disc cutter on the cutterhead should be recorded in the daily TBM cutter

Fig. 4 Views of TBM cutterhead and cutter arrangement on the cutterhead. **a** View of TBM cutterhead at B portal. **b** Cutterhead with cutter numbers
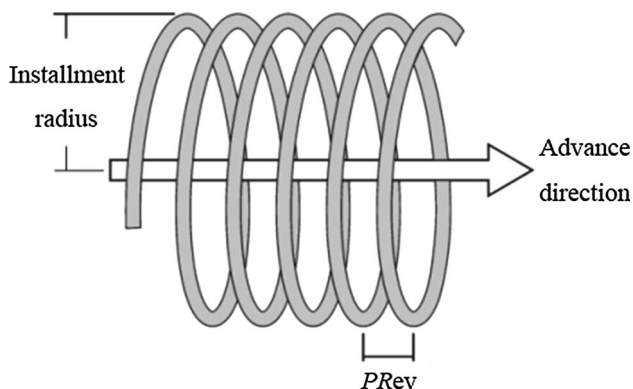

(a)

(b)

Fig. 6 Concentric circles on the tunnel face produced by disc cutters in this study

Fig. 7 Movement track of each disc cutter (modified from Frenzel 2011)

maintenance sheet during the daily maintenance of the machine. In addition, the allowable wear limit of the disc cutter is different based on the position and type of disc cutter. Therefore, the rock excavation volume per cutter wear extent or E_f (m^3/mm), calculated simply from the whole cutterhead perspective, is recommended, as indicated in Eq. (1), to evaluate the disc cutter life in this study.

$$E_f = \frac{\pi \cdot D^2 \cdot L}{4 \cdot M} \tag{1}$$

where D is the tunnel diameter (m), L is the excavated tunnel length (m), and M is the total wear extent of all disc cutters used on the cutterhead (mm), including the normal wear extent and abnormal wear extent.

The TBM utilization and daily advance are both lower when there is more downtime for machine maintenance. The cutter inspectors may only verify the condition of the disc cutters to ensure no abnormal wear as the cutters work continuously on the cutterhead, and the wear extent of every disc cutter is not measured during the daily
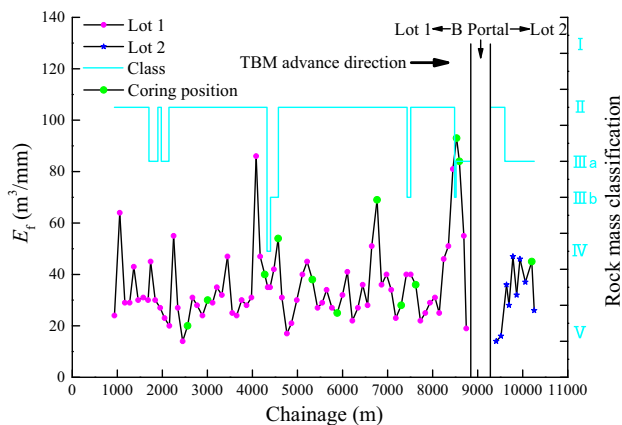
Fig. 8 Variations in the calculated average cutter life E_f along the two lots of the studied project

maintenance of the machine. Hence, at this moment, it will not be possible to obtain the daily cutter life E_f. Additionally, since the wear measurements have been taken with a manual gage, random errors and outliers can be encountered (Frenzel et al. 2008). To guarantee the accuracy of the calculation results, the average cutter life E_f of a tunnel section with a length of approximately 100 m and the same rock mass classification is calculated, and if the rock mass classification changes significantly, a new tunnel section will automatically be allocated. Due to the influence of the learning effect and machine debugging process in TBM tunneling, the daily TBM cutter maintenance sheets obtained in the first 2 months are excluded. Therefore, the time span of the collected data is from April 26, 2014 to September 9, 2015, with no daily TBM cutter maintenance sheet recorded for the overhaul of the TBM at the B portal from April 22, 2015 to July 9, 2015. All of the collected data were summarized in an Excel spreadsheet and compiled in a database. The variation of the average cutter life E_f along the two lots of the studied project is shown in Fig. 8 after the statistical analysis of the collected data. It can be seen that most of the calculated average cutter life values E_f are distributed in the range of 20–45 m^3/mm, and the maximum value is approximately 6.7 times the minimum value.

5 Wear Rule of 20-in. Disc Cutter

Disc cutter wear, including normal and abnormal wear, is one of the results of the rock–machine interaction in TBM tunneling. Normal wear refers to uniform wear along the circumferential direction of the cutter ring, as shown in Fig. 9, which is not only the most common form of cutter wear but also the main source of the cutter cost. Abnormal wear refers to all cutter failure modes except for normal

wear, including flat wear of the cutter ring, cracking or fracturing of the cutter ring, dropping out of the split ring, and spalling of the cutter ring. Flat wear of the cutter ring includes unilateral flat wear and polygonal flat wear and refers to the flattening of the cutter ring due to cutter rotation stoppage. Unilateral flat wear, as shown in Fig. 10a, refers to the unilateral flattening of the ring when the cutter does not rotate again after the rotation stoppage. Polygonal flat wear, as shown in Fig. 10b, refers to the polygonal flattening of the ring when cutter rotates again if a unilateral flattening of the ring does not develop too wide to hinder cutter rotation (Zhao et al. 2007). Cracking of the cutter ring, as shown in Fig. 10c, refers to a crack that appears along the radial direction. When multiple cracks emerge at different positions of the cutter ring at the same time, it is referred to as fracturing of the cutter ring. Dropping out of the split ring, as shown in Fig. 10d, refers to the fracturing and loss of the split ring due to poor welding quality. Spalling of the cutter ring, as shown in Fig. 10e, refers to the local spalling of the cutter ring due to fatigue cracks. Errors in the heat treatment of the cutter rings and impact loads from metal debris can result in such spalling, in addition to highly variable local loadings (Frenzel 2011). The total number of replaced disc cutters is 1095 in the studied project, with 982 (accounting for approximately 89.68%) were replaced for normal wear and 113 (approximately 10.32%) were replaced for abnormal wear, as shown in Fig. 11. This may be because of the high intactness degree of the rock mass in the studied project, leading to the local collapse of rocks on the tunnel face and large-size mucks being rare phenomena. Therefore, the probability of collision with an instantaneous high dynamic load between the disc cutters and rocks on the tunnel face

or large-size mucks is also low, such that normal wear plays a major role in the disc cutter wear.

The disc cutter needs to be replaced when the cutter ring reaches its allowable wear limit. Considering the limited disc cutter reserve and the common practice that the difference in the cutter ring wear extent between adjacent cutters should be less than 15 mm, the installed cutters may either be new ones or worn ones for adjustment. In addition, during the daily maintenance of the machine, the inspection of the disc cutter conditions includes the examination of the pre-torque and temperature, the measurement of the wear extent of the cutter rings, and the detection of the presence of abnormal wear. Disc cutters with an improper pre-torque or high temperature, implicating the occurrence of abnormal wear, must be removed from the cutterhead and then subjected to a postmortem inspection in the field cutter housing. In general, improper pre-torque or high temperature was judged through the manual rotation of the cutter ring based on the experience of the cutter inspectors. In the studied project, among the 982 disc cutters with normal wear, 516 worn disc cutters (approximately 52.55%) and 431 new disc cutters (approximately 43.89%) were installed to replace cutters reaching their wear limit, 32 disc cutters (approximately 3.26%) were installed to replace cutters with an improper pre-torque, and 3 disc cutters (approximately 0.31%) were installed to replace cutters with high temperature, as shown in Fig. 12.

The influence of a disc cutter with abnormal wear on the TBM tunneling is much more severe than that of a disc cutter with normal wear. If a disc cutter with abnormal wear, which must be replaced, is detected in the routine downtime after every 3–4 excavation strokes, it would greatly affect the normal TBM tunneling and reduce the TBM utilization. The failed internal components of the disc cutter such as the bearing or seal may cause abnormal wear, which would increase the cutter cost. An extreme example is that when an undetected failed cutter propagates damage to the surrounding cutters, the disc cutters may failed as a group (called a "wipeout" phenomenon), which may result in severe damage to the cutterhead even, and the resulting damage can take days or weeks to repair (Roby et al. 2008). In the studied project, among the 113 disc cutters with abnormal wear, 66 (approximately 58.41%) were replaced for flat wear of the cutter ring, including unilateral flat wear and polygonal flat wear, 42 (approximately 37.17%) were replaced for cracking or fracturing of the cutter ring, 1 (approximately 0.88%) was replaced for dropping out of the split ring, 2 (approximately 1.77%) were replaced for spalling of the cutter ring, and 2 (approximately 1.77%) were replaced for cracking of the hub, as shown in Fig. 13.
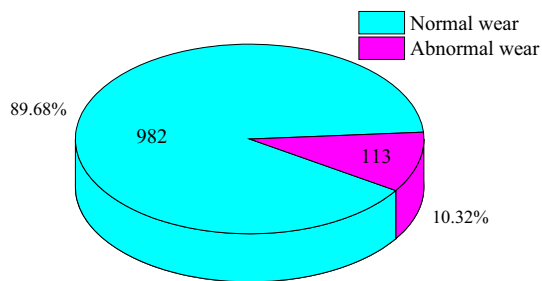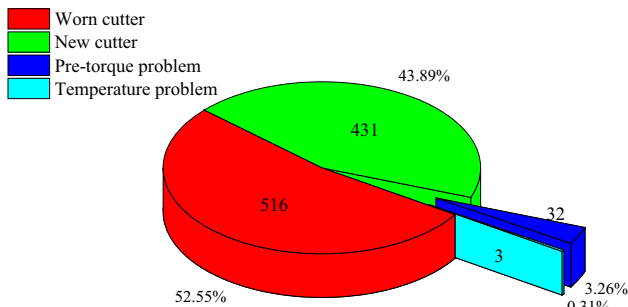

Fig. 9 Normal wear of disc cutter
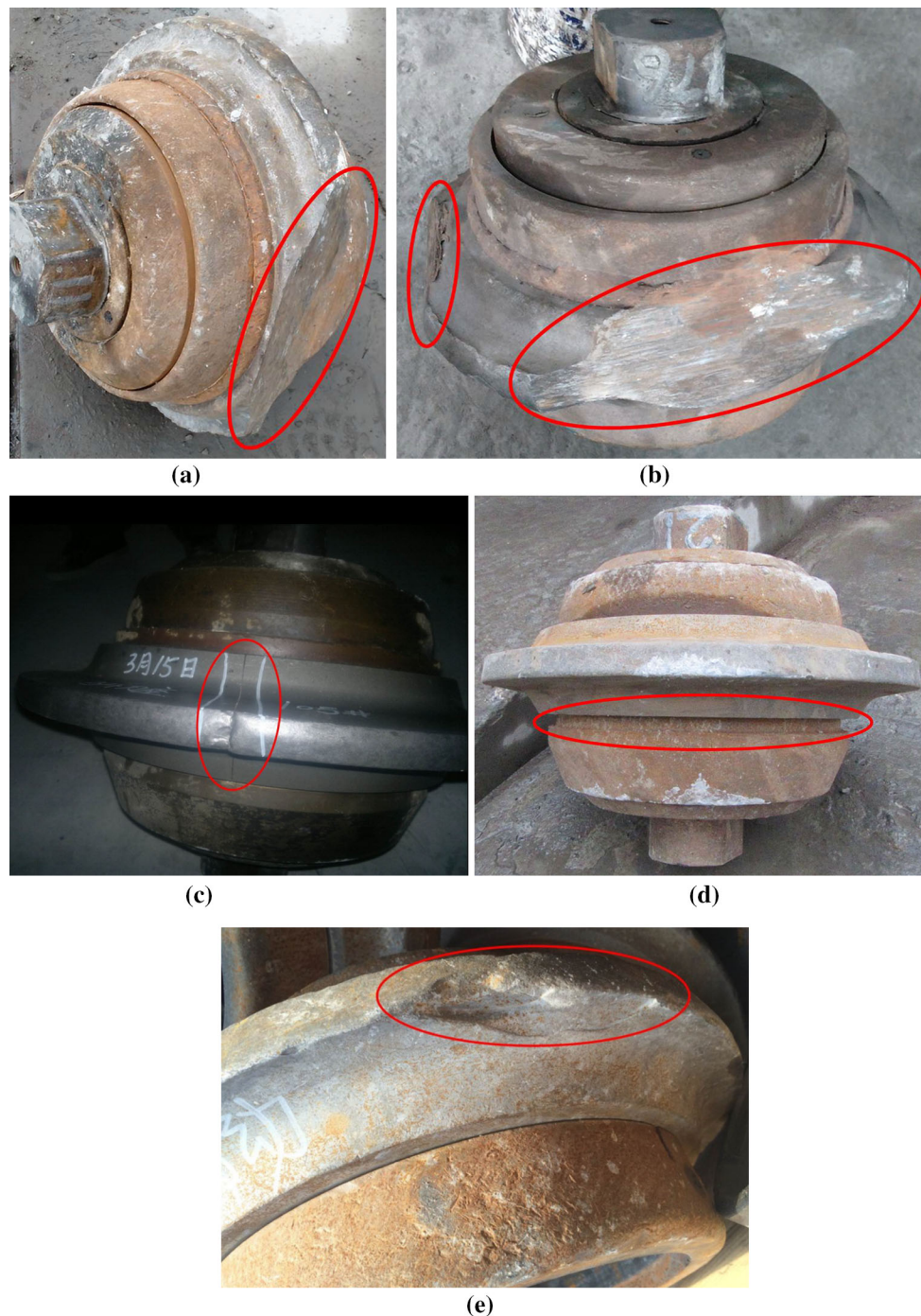
Fig. 10 Abnormal wear of disc cutters. **a** Unilateral flat wear of cutter ring. **b** Polygonal flat wear of cutter ring. **c** Cracking of cutter ring. **d** Dropping out of split ring. **e** Spalling of cutter ring

The total numbers of replaced center cutters, face cutters, and gage cutters are 55, 537, and 501 in the studied project, respectively. The histogram of the total number of disc cutter changes for each cutter position on the cutterhead is shown in Fig. 14. It can be seen that the number of disc cutter changes increases with the distance to the center of the cutterhead, as expected. The minor differences between the numbers of disc cutter changes for each cutter position can be observed for the center cutters. The number of changes in face cutters increases approximately linearly with the cutter position. Strictly speaking, disc cutters Nos. 44–51 should be referred to as transition cutters, and they change at more or less the same rate. The installment radiuses of gage cutters Nos. 52 and 53 are both the maximum and the linear velocities, but the

Fig. 11 Pie chart of normal wear and abnormal wear of disc cutter in the studied project
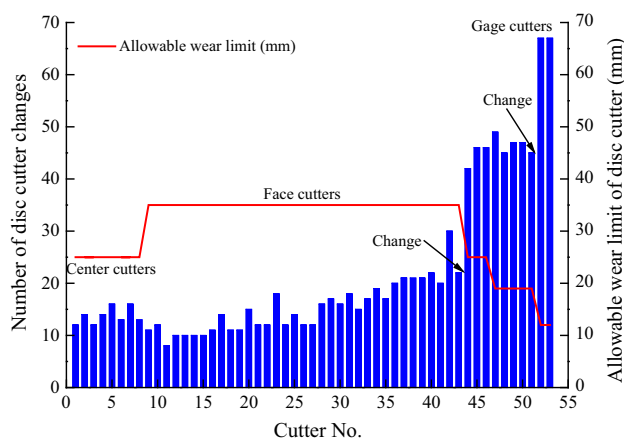

Fig. 12 Variations of normal wear of disc cutter in the studied project
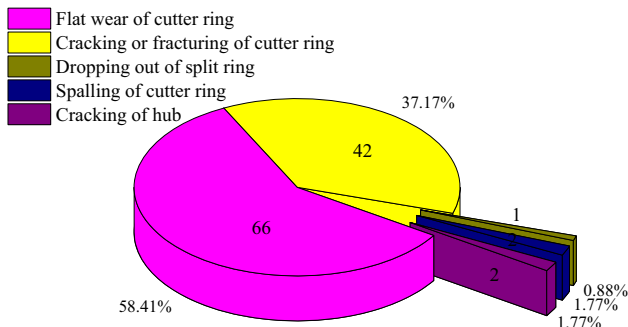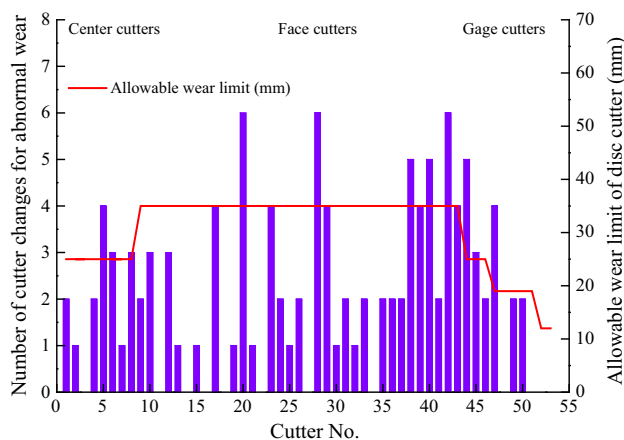

**Fig. 13** Variations of abnormal wear of disc cutter in the studied project

Fig. 14 Histogram of disc cutter changes in the studied project

Fig. 15 Histogram of disc cutter changes for abnormal wear in the studied project

allowable wear limits of these two cutters are both the minimum, such that they have the most changes. The correlation of these two cutters is strong for the same cutting track, and one failed disc cutter will propagate damage to the other (causing a "chain reaction") (Wei and Sha 1999), such that these two cutters need to be replaced at the same time. In addition, it can be seen in Fig. 14 that when the allowable wear limit of the disc cutter changes, the number of replaced disc cutters of the corresponding interface also changes, especially at the interfaces between the face cutter and transition cutter and between the transition cutter and gage cutter.

The histogram of disc cutter changes due to abnormal wear in the studied project is shown in Fig. 15. It can be seen that the number of replaced disc cutters for abnormal

wear is independent of the cutter position, which may be due to the anisotropy of the rock mass. In addition to the quality of the disc cutter, the abnormal wear is also related to the operation level of the TBM driver and the fracture degree of the rock mass.

The accumulated wear extent of the rings for the center cutters, face cutters, and gage cutters is 847, 8178, and 7410 mm, respectively. The histogram of the accumulated wear extent of the rings at each position on the cutterhead is shown in Fig. 16. It can be seen that the accumulated wear extent of the rings for the center cutters and face cutters roughly increased linearly with the distance to the center of the cutterhead. For gage cutters, there is a sudden increase in the accumulated wear extent. This is mainly because the mucks produced by the cutter cutting fail to be discharged from the buckets in time when the TBM penetration rate is too fast, which gives rise to secondary wear of the cutter rings, which leads to a rapid increase in the accumulated wear extent of the rings of the gage cutters. The accumulated wear extent of the rings of different types
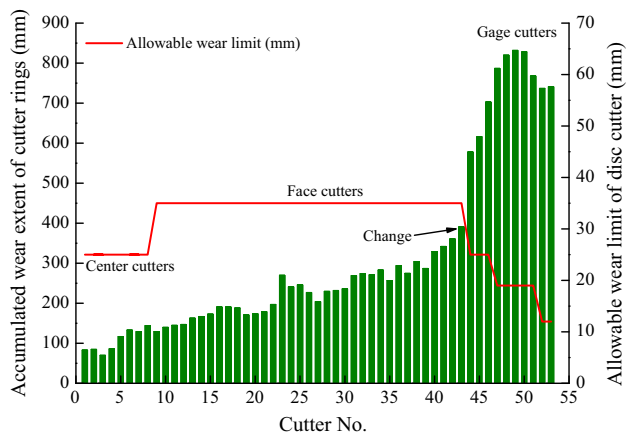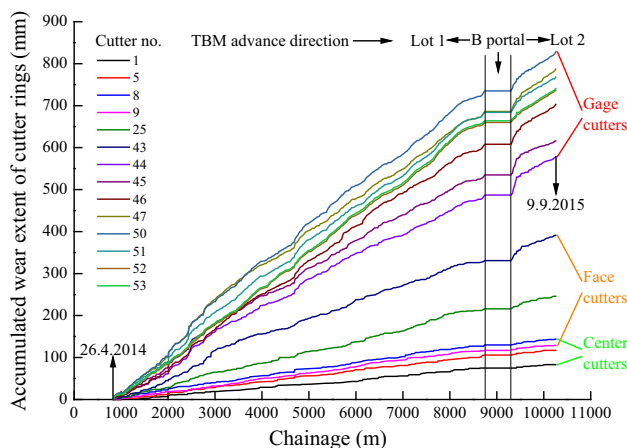
Fig. 16 Histogram of the accumulated wear extent of the rings in the studied project

of cutters along the two lots of the studied project is shown in Fig. 17.

6 Development of New Empirical Relationships

The main purpose of this study is to develop a new cutter life prediction model for a 20-in. disc cutter in granite. However, disc cutter wear is a very complex process that is not yet fully understood (Thuro and Käsling 2009). It is well known that many factors affect the disc cutter life, including the properties of the intact rock, parameters of the rock mass, and quality of the disc cutter. Fortunately, disc cutters manufactured by Robbins Company of high quality were employed in the whole studied tunnel. The histogram of the calculated average cutter life E_f variation in the surrounding rock of class II (see Table 3) shown in Fig. 18 indicates that the disc cutter life cannot be predicted accurately using rock mass classification systems.
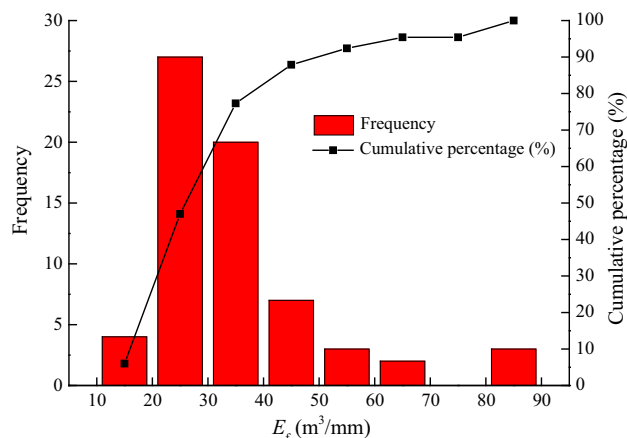
This is mainly because the existing rock mass classification systems were developed based on the stability analysis of the surrounding rock and do not yet consider the main factors influencing the disc cutter life, e.g., the Cerchar abrasivity index. As mentioned before, the surrounding rock of class II accounts for the majority, and the distribution ranges of the rock mass intactness degree and weathering degree are relatively narrow in the studied tunnel. Therefore, this research focuses on the empirical relationships between the intact rock parameters and the disc cutter life.

6.1 Data Collection

The variation of the average cutter life E_f along the studied tunnel shown in Fig. 8 is determined by the statistical analysis of the daily TBM cutter maintenance sheets generated in the construction phase. Considering the distribution characteristics of the average cutter life, the uniform distribution of coring positions, and the operability of field conditions, the rock corings for the laboratory tests, including the Cerchar abrasivity test, uniaxial compressive strength test, and X-ray diffraction test, were conducted at 12 representative positions along the studied tunnel (see Fig. 8).

The Cerchar abrasivity test is a laboratory test method commonly used for assessing the rock abrasivity due to its simple setup and easy operational procedure (Ho et al. 2016). The tests should be carried out on "broken" and even surfaces according to the corresponding testing recommendations. However, no suitable rock surfaces can be obtained by breaking the inhomogeneous coarse-grained granites with a hammer or other splitting device. Therefore, rock samples with "smooth" surfaces for the Cerchar abrasivity tests with a West-type apparatus using a stylus with a Rockwell hardness HRC 54–56 (Alber et al. 2014)

Fig. 17 Accumulated wear extent of the rings of different types of cutters along the two lots of the studied project

Fig. 18 Histogram of the calculated average cutter life E_f variation in the surrounding rock of class II

were obtained by cutting using a water-cooled diamond saw. The tests were conducted at the Beijing University of Technology, and the results were corrected with the recommended Eq. (2) suggested by Plinninger et al. (2003). The arithmetic average value of 5 Cerchar abrasivity tests was used to represent the abrasivity of the corresponding rock, and the results show that most of the CAI values of the granite are in the range of 3.8–4.5 in this study.

$$CAI = 0.99CAI_s + 0.48 \qquad (2)$$

where CAI is the Cerchar abrasivity index of a rock sample with a "rough" surface, and CAI_S is the Cerchar abrasivity index of a rock sample with a ''smooth'' surface.

The rock strength also has an important influence on the cutter wear. Thus, uniaxial compressive strength tests were carried out on rock samples in accordance with the National Standards Compilation Group of People's Republic of China (2007) with an RMT-301 apparatus at the Wuhan University. As the diameter of the rock sample is not the standard size, namely 50 mm, the measured σ_{cd} is corrected to the strength for a standard sample with a diameter of 50 mm using Eq. (3) proposed by Hoek and Brown (1997), and the results show that the σ_{c50} values of the granite are in the range of 40–100 in this study.

$$\sigma_{c50} = \sigma_{cd} \left(\frac{d}{50} \right)^{0.18} \qquad (3)$$

where σ_{c50} is the uniaxial compressive strength of a rock sample with a diameter of 50 mm (MPa) and σ_{cd} is the uniaxial compressive strength of a rock sample with a diameter of d mm (MPa).

The rock abrasivity is the comprehensive performance of various mineral compositions, influenced by the mineral hardness, rock texture, grain size and shape, cement type, and degree. Currently, there are two commonly used methods for quantitatively determining the mineral composition of rock samples, namely thin-section analysis and X-ray diffraction analysis. Modern diffractometers are capable of relatively fast and reliable identification and quantification of the mineral content by use of PC-guided systems (Plinninger 2010). Therefore, X-ray diffraction analysis was employed in this study. An X-ray diffraction pattern was obtained by irradiating X-rays on the powdered sample at different incident angles. To obtain a qualitative result of the mineral composition, the position and intensity of the peaks in the pattern were analyzed by use of PC-guided systems. Subsequently, the quantitative result of the mineral composition was obtained by means of calculating the height and area of the peaks in the pattern. The analytical procedure is automatic after the powdered sample preparation. The powdered sample passing through a 200-mesh sieve and being selected by the quartering sampling technique can guarantee the representativeness,

authenticity, and repeatability of the XRD test result. In this study, a D8 Advance X-ray diffractometer at the Institute of Rock and Soil Mechanics was employed to obtain the X-ray diffraction patterns of the different powdered samples, as shown in Fig. 19. The results show that the main mineral constituents of the granite are microcline, quartz, clinochlore, albite, and muscovite. It is a well-known fact that tool wear is caused by contact with a mineral of a hardness greater than that of steel (Mohs hardness approximately 5.5), particularly quartz (Mohs hardness 7.0) (Thuro 1997). To consider the influence of all of the minerals on tool wear, it is necessary to introduce the concept of equivalent quartz content, which can be calculated using Eq. (4) proposed by Thuro (1997), and the results show that EQC values of the granite are in the range of 20–50% in this study.

$$EQC = \sum_{i=1}^{n} A_i \cdot R_i \qquad (4)$$

where EQC is the equivalent quartz content (%), A_i is each mineral constituent of the rock sample (%), R_i is the Rosiwal hardness referred to quartz (100), and n is the total number of minerals in the rock sample.

The rock abrasivity index (RAI), modified from the equivalent quartz content (EQC), was first presented in the course of the 9th IAEG Congress in Durban, South Africa (Plinninger et al. 2002), and it considers the content of abrasive minerals as well as the strength of the rock. RAI has been proven to be an ideal parameter for the characterization and classification of the hard rock abrasivity for its accessible input parameters and simple calculation using Eq. (5) proposed by Plinninger (2010), and the results show that the RAI values of the granite are in the range of 10–45 in this study.
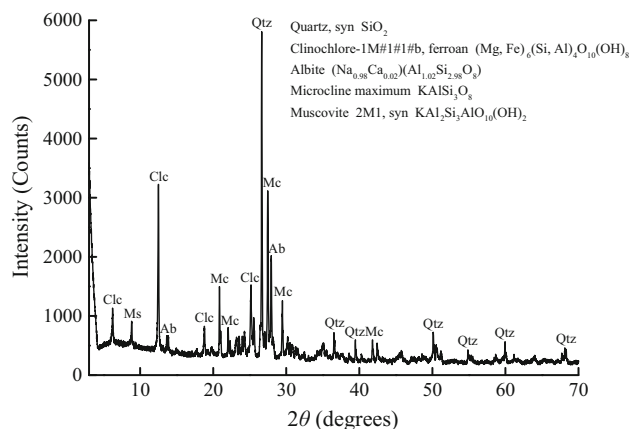

Fig. 19 X-ray diffraction pattern obtained from the powdered sample 1

$$RAI = EQC \cdot UCS = \sum_{i=1}^{n} A_i \cdot R_i \cdot UCS \qquad (5)$$

where RAI is the rock abrasivity index and UCS is the unconfined compressive strength (MPa), namely σ_{c50}.

The database employed for the 20-in. TBM cutter life prediction consists of 12 datasets from 12 tunnel sections. Table 5 lists the ranges and average values of the cutter life (E_f) and intact rock properties, including the Cerchar abrasivity index (CAI), uniaxial compressive strength (UCS), quartz content (Q), equivalent quartz content (EQC), and rock abrasivity index (RAI).

6.2 Statistical Analyses

Empirical equations based on geomechanical or operating parameters have been widely used for predicting target parameters in geotechnical engineering. As stated by Hassanpour et al. (2014): ''empirical equations have higher importance during the early stages of design since they are more practical and based on actual projects, compared to extensive theoretical analyses.'' Therefore, both simple regression and multiple regression analyses were used to derive the relationships between the average cutter life and intact rock parameters.

6.2.1 Simple Regression Analysis

A simple empirical relationship between a target variable and a single independent variable can be established using simple regression analysis for a rough estimate of the target variable in similar ground conditions. Figure 20 shows simple empirical relationships between E_f and different

intact rock properties including CAI, UCS, Q, EQC, and RAI. Table 6 summarizes the type, equation, and determination coefficient of the optimal empirical relationships. As shown, there is a poor correlation ($R^2 = 0.191$) between the quartz content and cutter life, which indicates that the disc cutter life cannot be estimated accurately using the quartz content alone. By considering the influence of all of the minerals on the cutter wear, the determination coefficient R^2 between the equivalent quartz content and cutter life increases significantly to 0.689. Moreover, by considering the influence of the mineral composition and rock strength on the cutter wear, the rock abrasivity index shows a better correlation with the cutter life ($R^2 = 0.874$). Hence, the cutter life of a 20-in. disc cutter used in granite can be predicted roughly using the empirical Eq. (10). Strong correlations between the Cerchar abrasivity index and uniaxial compressive strength and the cutter life, with $R^2 = 0.847$ and 0.834, respectively, are also established.

6.2.2 Multiple Regression Analysis

The multiple regression analysis was used to find an empirical equation with the best fit to the existing data. A professional statistical analysis software (SPSS) was employed for predicting the cutter life in this study. According to the results of the simple regression analysis, two intact rock properties including CAI and UCS were input as dependent variables, and the calculated average cutter life (E_f) was chosen as the independent variable. The influence of each variable on E_f was evaluated using forward stepwise regression analyses, which can generate different models with input variables as shown in Table 7. In these models, the maximum determination coefficient

Table 5 Intact rock parameters and calculated average cutter life along the studied project

No.	Chainage (m)	Lithotype	CAI		UCS (MPa)		Q (%)	EQC (%)	RAI		E_f (m³/mm)
			Range	Average	Range	Average			Range	Average	
1	10,191	Granite	3.8–4.2	4.0	70–80	75	13	32	22–26	24	45
2	8592	Andesite	2.0–3.6	2.6	40–50	45	9	22	9–11	10	84
3	8530	Granite	0.8–2.8	1.8	35–45	40	24	28	10–14	12	93
4	7588	Granite	4.1–5.1	4.5	50–80	65	30	49	24–40	32	36
5	7298	Granite	3.7–4.2	4.0	75–85	80	14	35	27–30	29	28
6	6740	Granite	1.4–4.0	2.9	25–45	35	12	27	7–12	10	70
7	5828	Granite	3.4–4.7	4.3	75–90	85	24	39	29–35	33	25
8	5283	Granite	3.7–5.1	4.3	60–75	65	17	37	22–28	25	38
9	4491	Granite	3.6–4.4	4.0	45–65	55	12	27	12–17	15	54
10	4272	Granite	3.5–4.2	3.8	55–70	65	19	39	21–29	25	40
11	2923	Granite	3.6–4.9	4.0	85–95	90	19	43	36–40	38	30
12	2581	Granite	4.0–4.7	4.2	90–105	95	27	44	40–47	43	20
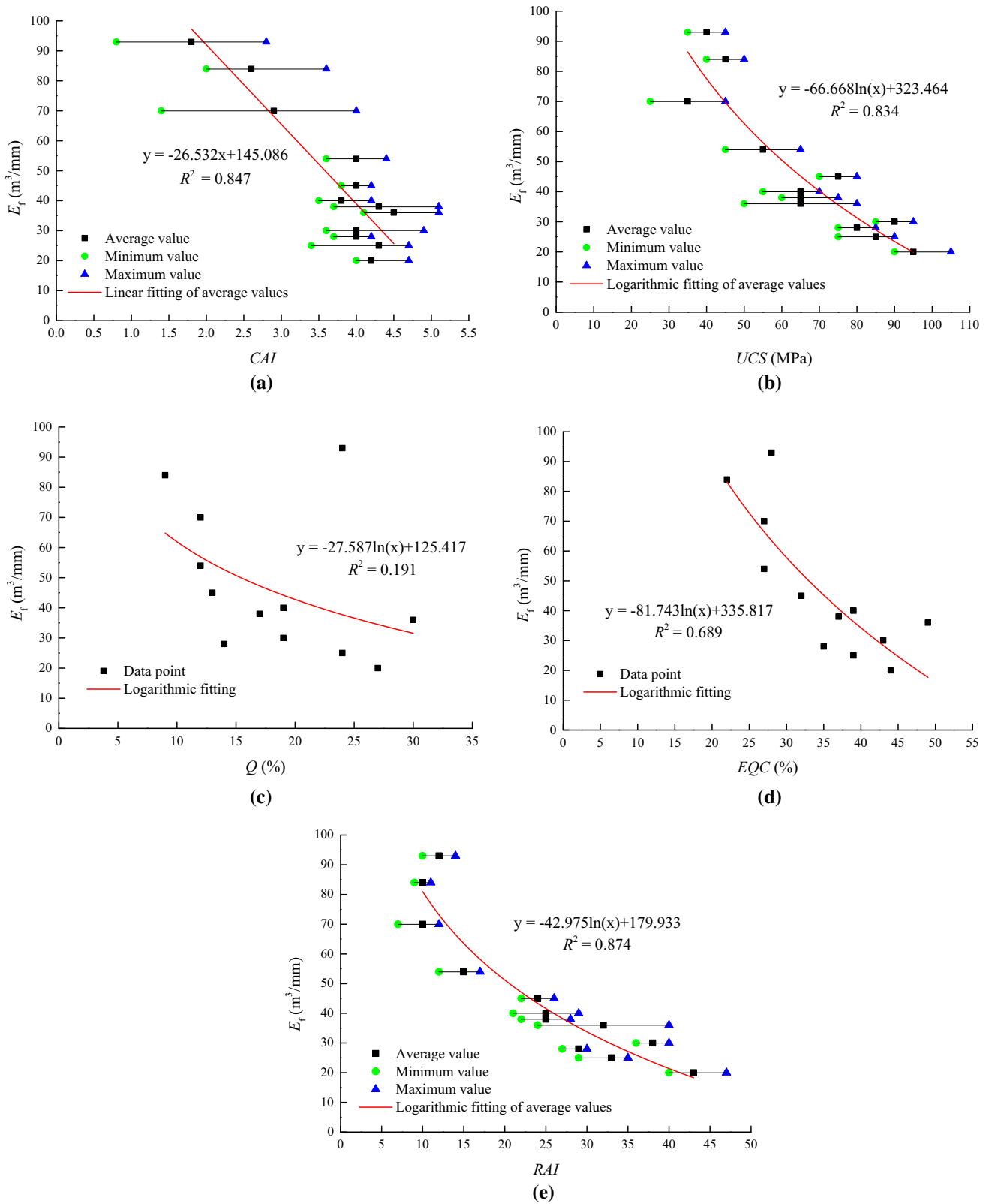
Fig. 20 Relationships between the calculated average cutter life E_f and different intact rock parameters. **a** CAI and E_f. **b** UCS and E_f. **c** Q and E_f. **d** EQC and E_f. **e** RAI and E_f

Table 6 Summary of relationships between different intact rock parameters and cutter life

Dependent variable	Independent variable	Function type	Equation	Determination coef. (R^2)	Eq. no.
E_f (m³/mm)	CAI	Linear	$E_f = -26.532 \, CAI + 145.086$	0.847	(6)
	UCS (MPa)	Logarithmic	$E_f = -66.668 \, Ln(UCS) + 323.464$	0.834	(7)
	Q (%)	Logarithmic	$E_f = -27.587 \, Ln(Q) + 125.417$	0.191	(8)
	EQC (%)	Logarithmic	$E_f = -81.743 \, Ln(EQC) + 335.817$	0.689	(9)
	RAI	Logarithmic	$E_f = -42.975 \, Ln(RAI) + 179.933$	0.874	(10)

Table 7 Variables and summary of the generated models for forward stepwise regression analysis

Model	Variables entered	Variables removed	Method
1	CAI		Stepwise (criteria: probability-of-F-to-enter ≤ 0.050, Probability-of-F-to-remove ≥ 0.100)
2	UCS		Stepwise (criteria: probability-of-F-to-enter ≤ 0.050, probability-of-F-to-remove ≥ 0.100)

Model summary	R	R square	Adjusted R square	SE of the estimate
1	0.921[a]	0.847	0.832	9.71313
2	0.976[b]	0.953	0.943	5.67656

Dependent variable: E_f

[a] Predictors: (constant), CAI

[b] Predictors: (constant), CAI, UCS

($R^2 = 0.953$) was obtained in model 2, which selected CAI and UCS as input variables. Consequently, the best fit regression between the input parameters in a linear combination with a 95% confidence level was obtained using multiple regression analysis. As a result, a new 20-in. disc cutter life prediction model, as illustrated in Table 8, was empirically obtained as follows:

$$E_f = -16.079 CAI - 0.587 UCS + 145.295 \qquad (11)$$

To test the utility of the overall regression model, the analysis of variance (F test), as shown in Table 9, was conducted. The statistical values F and Sig. of model 2 are 91.407 and 0.000, respectively. Therefore, the null hypothesis can be rejected, which means that at least one of the independent variables can significantly affect E_f. Moreover, the t test shown in Table 8 indicates that the coefficients of model 2 are true.

To evaluate the accuracy of the developed model, a comparison of the measured and predicted values of E_f is shown in Fig. 21. As shown, most of the residuals are less than 10 m³/mm.

A cutter life prediction chart of the 20-in. disc cutter derived from Eq. (11) is developed and shown in Fig. 22 for convenient and practical application. The 12 data points including the corresponding ranges have been plotted. The approximate range of E_f can be estimated quickly using Fig. 22 in grounds with different rock strength and rock abrasivity values. However, it must be emphasized that the influences of the rock mass parameters, weathering degrees, and in situ stresses on the disc cutter life are not considered in the developed models, and these proposed empirical relationships should be considered valid only for new projects with geological conditions and machine specifications similar to those of the tunnel studied in this study. More field data from different projects need to be collected to develop a universal model that can be applicable to other rock types and machine specifications.

7 Conclusions

Field data from a water conveyance tunnel through granite in China were used to reveal the genuine wear rule of a 20-in. disc cutter and develop reasonable correlations between some common intact rock parameters and the disc cutter life. The results show that normal wear plays a major role in the disc cutter wear, and the number of disc cutter changes and the accumulated wear extent of the rings increase with the distance to the center of the cutterhead for center cutters and face cutters, while those for gage cutters are larger due to the lower allowable wear limits and secondary wear of the cutter rings. The number of replaced disc cutters for abnormal wear is independent of the cutter position.

Table 8 Coefficients and t test for each generated model

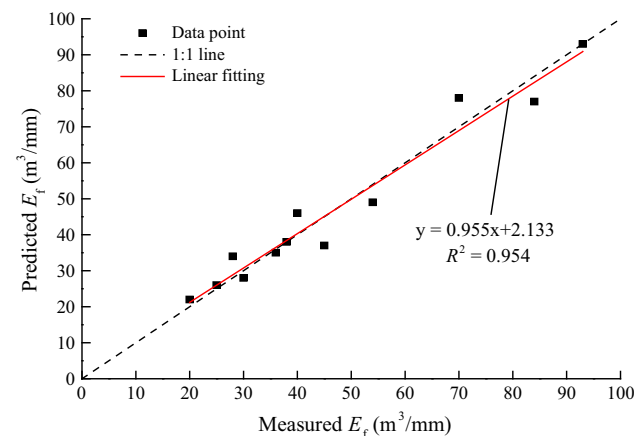| Model	Unstandardized coefficients		Standardized coefficients	t	Sig.
	B	SE	Beta		
1					
(Constant)	145.086	13.471		10.770	0.000
CAI	−26.532	3.561	−0.921	−7.451	0.000
2					
(Constant)	145.295	7.873		18.455	0.000
CAI	−16.079	3.118	−0.558	−5.157	0.001
UCS	−0.587	0.130	−0.487	−4.503	0.001

Dependent variable: E_f

Table 9 Analysis of variance for the significance of regression for each generated model

Model	Sum of squares	df	Mean square	F	Sig.
1					
Regression	5237.468	1	5237.468	55.514	0.000[a]
Residual	943.449	10	94.345		
Total	6180.917	11			
2					
Regression	5890.906	2	2945.453	91.407	0.000[b]
Residual	290.010	9	32.223		
Total	6180.917	11			

Dependent variable: E_f

[a] Predictors: (constant), CAI

[b] Predictors: (constant), CAI, UCS

Fig. 22 Average cutter life prediction chart for granite based on the intact rock parameters derived from Eq. (11)

Fig. 21 Comparison of the measured and predicted values of average cutter life

A poor correlation between the quartz content and cutter life is found, a moderate correlation between the equivalent quartz content and cutter life is identified, strong relationships between the Cerchar abrasivity index and uniaxial compressive strength and the cutter life are established, and

the rock abrasivity index has the best correlation with the cutter life. A new 20-in. disc cutter life prediction model with a determination coefficient R^2 of 0.953 was empirically obtained, which selected CAI and UCS as the input variables.

It needs to be stressed that the influences of the rock mass parameters, weathering degrees and in situ stresses on the disc cutter life are not considered in the developed models, and the proposed relationships should be applied with caution and considered valid only for similar geological conditions and TBM specifications. These equations were developed based on data from massive to very massive granite with a UCS range of 40–100 MPa. It is not recommended to use these models for faults, tectonic activities, and shear zones as well as zones with special geological conditions including mixed and interfaced grounds, spalling and bursting rocks, or blocky and highly fractured rocks. In addition, more field data from different projects need to be collected to extend the models developed in this study, and a universal model applicable for various geological conditions and machine specifications will be developed in the future.

References

Alber M, Yaralı O, Dahl F, Bruland A, Kasling H, Michalakopoulos TN, Cardu M, Hagan P, Aydın H, Ozarslan A (2014) ISRM suggested method for determining the abrasivity of rock by the CERCHAR abrasivity test. Rock Mech Rock Eng 47:261–266. doi:10.1007/s00603-013-0518-0

Bieniawski ZT (1989) Engineering rock mass classifications. Wiley, New York

Bieniawski ZT, Celada CB, Galera JM, Tardaguila IG (2009) Prediction of cutter wear using RME. ITA-AITES World Tunnel Congress, Budapest

Bruland A (1998) Hard rock tunnel boring. Dissertation, Norwegian University of Science and Technology

Dahl E, Grøv E, Breivik T (2007) Development of a new direct test method for estimating cutter life based on the Sievers' J miniature drill test. Tunn Undergr Space Technol 22:106–116. doi:10.1016/j.tust.2006.03.001

Du SB (2006) Advantages of tunnelling by TBM with large diameter disc cutter. Water Resour Hydropower Eng 37(10):40–42. doi:10.13928/j.cnki.wrahe.2006.10.012 (in Chinese)

Du LJ, Ji SS, Zuo LF, Kong HX, Xu JL, Du YL (2015) Wear and consumption of large diameter disc cutters for hard rock TBM under giant porphyritic granite. J China Coal Soc 40(12):2974–2978. doi:10.13225/j.cnki.jccs.2015.3042 (in Chinese)

Ewendt G (1992) Erfassung der Gesteinsabrasivität und Prognose des Werkzeugverschleißes beim maschinellen Tunnelvortrieb mit Diskenmeißeln. Kurzberichte aus der Bauforschung 33(9):821–822 (in German)

Frenzel C (2011) Disc cutter wear phenomenology and their implications on disc cutter consumption for TBM. In: 45th American Rock Mechanics/Geomechanics Symposium. San Francisco, USA

Frenzel C (2012) Modeling uncertainty in cutter wear prediction for tunnel boring machines. GeoCongress 2012: State of the Art and Practice in Geotechnical Engineering, pp 3239–3247

Frenzel C, Käsling H, Thuro K (2008) Factors influencing disc cutter wear. Geomech Tunn 1(1):55–60. doi:10.1002/geot.200800006

Gehring K (1995) Prognosis of advance rates and wear for underground mechanized excavations. Felsbau 13(6):439–448 (in German)

Hassanpour J, Rostami J, Azali ST, Zhao J (2014) Introduction of an empirical TBM cutter wear prediction model for pyroclastic and mafic igneous rocks; a case history of Karaj water conveyance tunnel, Iran. Tunn Undergr Space Technol 43:222–231. doi:10.1016/j.tust.2014.05.007

Ho YK, So STC, Lau TMF, Kwok RCM (2016) Abrasiveness of common rocks in Hong Kong. Rock Mech Rock Eng 49:2953–2958. doi:10.1007/s00603-015-0873-0

Hoek E, Brown ET (1997) Practical estimates of rock mass strength. Int J Rock Mech Min Sci 34(8):1165–1186. doi:10.1016/S1365-1609(97)80069-X

Jin YQ, Liu ZH, Yang L, Zheng GS (2011) Analyzing the cause of TBM disc cutter wear in Yintao project No.9 tunnel. Constr Mech 6:79–81. doi:10.13311/j.cnki.conmec.2011.06.022 (in Chinese)

Liu QS, Huang X, Gong QM, Du LJ, Pan YC, Liu JP (2016a) Application and development of hard rock TBM and its prospect in China. Tunn Undergr Space Technol 57:33–46. doi:10.1016/j.tust.2016.01.034

Liu QS, Liu JP, Shi K, Pan YC, Huang X, Liu XW, Wei L (2016b) Evaluation of rock brittleness indexes on rock fragmentation efficiency by disc cutter. Chin J Rock Mech Eng 35(3):498–510. doi:10.13722/j.cnki.jrme.2015.0569 (in Chinese)

Maidl B, Schmidz L, Ritz W, Herrenknecht M (2008) Hard rock tunnel boring machines. Wiley, New York

Nelson PP, Al-Jalil YA, Laughton C (1994) Tunnel boring project data bases and construction simulation. Geotechnical engineering report GR94-4, University of Texas at Austin

Plinninger RJ (2010) Hardrock abrasivity investigation using the Rock Abrasivity Index (RAI). In: Williams et al (eds) Geologically active. Taylor, London, pp 3445–3452

Plinninger RJ, Spaun G, Thuro K (2002) Prediction and classification of tool wear in drill and blast tunnelling. In: Proceedings of the 9th IAEG Congress, Durban, pp 2226–2236

Plinninger R, Kasling H, Thuroc K, Spaun G (2003) Testing conditions and geomechanical properties influencing the CERCHAR abrasiveness index (CAI) value. Int J Rock Mech Min Sci 40:259–263. doi:10.1016/S1365-1609(02)00140-5

Roby J, Sandell T, Kocab J, Lindbergh L (2008) The current state of disc cutter design and development directions. In: Proceedings of 2008 North American Tunnel Congress. San Francisco, USA, pp 36–45

Rostami J (1997) Development of a force estimation model for rock fragmentation with disc cutters through theoretical modeling and physical measurement of crushed zone pressure. Dissertation, Colorado School of Mines

Schneider E, Thuro K, Galler R (2012) Forecasting penetration and wear for TBM drives in hard rock–results from the ABROCK research project. Geomech Tunn 5(5):537–546. doi:10.1002/geot.20120

The National Standards Compilation Group of People's Republic of China (2007) DL/T5368–2007 Code for rock tests of hydroelectric and water conservancy engineering. China Planning Press, Beijing (in Chinese)

The National Standards Compilation Group of People's Republic of China (2009) GB50487–2008 Code for engineering geological investigation of water resources and hydropower. China Planning Press, Beijing (in Chinese)

Thuro K (1997) Prediction of drillability in hard rock tunnelling by drilling and blasting. In: World Tunnel Congress, Rotterdam, pp 103–108

Thuro K, Käsling H (2009) Classification of the abrasiveness of soil and rock. Geomech Tunn 2(2):179–188. doi:10.1002/geot.200900012

Wan ZC, Sha MY, Zhou YL (2002a) Study on disc cutters for hard rock (1)—Application of TB880E TBM in Qinling tunnel. Mod Tunnel Technol 39(5):1–11. doi:10.13807/j.cnki.mtt.2002.05.001 (in Chinese)

Wan ZC, Sha MY, Zhou YL (2002b) Study on disc cutters for hard rock (2)—application of TB880E TBM in Qinling tunnel. Mod Tunnel Technol 39(6):1–12. doi:10.13807/j.cnki.mtt.2002.06.001 (in Chinese)

Wang LH, Kang YL, Cai ZX, Zhang Q, Zhao Y, Zhao HF, Su PC (2012) The energy method to predict disc cutter wear extent for hard rock TBMs. Tunn Undergr Space Technol 28:183–191. doi:10.1016/j.tust.2011.11.001

Wei NZ, Sha MY (1999) The analysis of TBM cutter wear characteristic in the construction of Qinling tunnel.

J Shijiazhuang Rail Inst 12(2):86–89. doi:10.13319/j.cnki.sjztddxxbzrb.1999.02.023 **(in Chinese)**

Wijk G (1992) A model of tunnel boring machine performance. Geotech Geol Eng 10:19–40. doi:10.1007/BF00881969

Yang YD, Chen K, Li FY, Zhou JJ (2015) Wear prediction model of disc cutter. J China Coal Soc 40(6):1290–1296. doi:10.13225/j.cnki.jccs.2014.3037 **(in Chinese)**

Zhao ZX (2015) Research on the wear of TBM disc cutter during the excavating of the mountain tunnel. Chin J Undergr Space Eng 11(S1):367–372 **(in Chinese)**

Zhao J, Gong QM, Eisensten Z (2007) Tunnelling through a frequently changing and mixed ground: a case history in Singapore. Tunn Undergr Space Technol 22(4):388–400. doi:10.1016/j.tust.2006.10.002